Vietnam Journal of Mechanics, Vol. 45, No. 1 (2023), pp. 60 – 74
DOI: https://doi.org/10.15625/0866-7136/17938

DYNAMIC BUCKLING ANALYSIS OF REINFORCED COMPOSITE PLATE SUBJECTED TO HARMONIC LOADS

Pham Tien Dat[1,*], **Le Pham Binh**[1]
[1]*Military Technical Academy, Hanoi, Vietnam*
*E-mail: tiendat1962@gmail.com

Received: 06 December 2022 / Published online: 02 January 2023

Abstract. Composite plates are high-tech structures used in many areas of modern engineering, like building, space travel, ships, etc. In practice, these structures are often used in their thin form, typically a reinforced composite plate subjected to dynamic loads. Therefore, when subjected to loads, the plate may be instability. The article presents the element model, finite element algorithm, and buckling analysis results of reinforced composite plates subjected to dynamic loads in order to determine the buckling domain. Furthermore, the influence of some factors such as geometric parameters, reinforcing stiffeners, and material characteristics on the buckling domain of the plate is studied in detail.

Keywords: dynamic buckling, composite plate, harmonic loads.

1. INTRODUCTION

Research on the parameter stability of the structure has been carried out by many scientists. Among them, the earliest Bolotin [1] has had many research results on the parameter stability of elastic systems such as isotropic homogeneous plates and shells subjected to harmonic loads. Sofiyev et al. [2] solved the problem of bending plates and shells under the action of torsion forces that change linearly with time. The authors established the stability equation as a system of differential equations with time-dependent coefficients solved by applying Galerkin's method, and established formulas for limited dynamic and static loads. Hutt and Salam [3] used the finite element method to analyze the dynamic stability of homogeneous plates using a four-node thin plate element, which gave results on the dynamic stability of rectangular plates subjected to dynamic loads with or without shock absorbers. Aboudi et al. [4] studied the instability of homogeneous, viscous plates under cyclic compressive loads in the plane on the basis of Liapunov exponents, thereby establishing formulas for dynamic loads. Srinivasan and

Chellapandi [5] used the analytical method to investigate the dynamic stability of a rectangular plate bearing harmonic load on the plate's mean surface, determine the expression of the critical force, and construct graphs of the plate's stability domain.

The increasing use of fiber-reinforced composite panels and shells in many important engineering fields has led to interest in the influence of the material structure on the dynamic instability of the structure. Therefore, the study of dynamic stability calculation of structures made of composite materials is also of interest to many scientists. The dynamic instability of composite panels under compressive loads in the plane is studied in [6], in which author Cederbaum built the basic equations and used the Bubnov–Galerkin method to calculate Calculate and investigate the influence of some geometrical and material factors on the critical force. Chen and Yang [7] investigated the dynamic stability of a composite rectangular plate uniformly compressed at the mean and flexural surfaces using the Galerkin method. The research results show that the influence of horizontal shear deformation and rotational inertia as well as the influence of the number of layers, reinforcement angle, and load characteristics on the critical parameters are clear. Wang and Dawe [8] have investigated the dynamic stability characteristics of rectangular composite plates using Bolotin's method, where periodic solutions in the form of Fourier series are employed, and the boundaries of the instability regions are obtained using eigenvalue approach. Grady et al. [9] presented the results of studying the dynamic stability of layered composite panels subjected to impact loads by the finite element method. The authors have built a dynamic stability equation and a solution algorithm. Through the study, the influence of the composite layer on the unstable forms was investigated. Sahoo and Singh [10] studied the dynamic stability of layered composite panels and sandwich panels subjected to harmonic compression in the mean face of the plate. Using the finite element method, algorithms and numerical simulations have been built to allow the study of the influence of geometrical parameters, materials, boundary conditions, and loads on the critical force of the structure. Dey and Singha [11], the dynamic stability characteristics of simply supported laminated composite skew plates subjected to a periodic in-plane load are investigated using the finite element approach. The formulation includes the effects of transverse shear deformation, in-plane and rotary inertia. The boundaries of the instability regions are obtained using the Bolotin's method and are represented in the nondimensional load amplitude-excitation frequency plane. The principal and second instability regions are identified for different parameters such as skew angle, thickness-to-span ratio, fiber orientation and static in-plane load. Moorthy et al. [12] studied the dynamic instability of composite panels subjected to bidirectional compressive loads in the mean plane by analytical method. Dynamic instability behavior of composite and sandwich laminates with interfacial slips was studied by Chakrabarti and Sheikh [13], by using the refined higher order shear deformation theory and later the same theory combined with a linear spring model was used to study the dynamic instability of imperfect laminated sandwich plates having in-plane partial edge loading. This paper reports on the dynamic instability study conducted on symmetric angle-ply composite plate. The FEM formulation used in this study is based on the first order shear deformation theory (FSDT). The instability charts are plotted and the effect of several parameters on the instability chart and the degree of instability (DOI) have been calculated.

To enhance the stability of the plate, the solution of arranging reinforcement ribs was used. One of the current research topics is the numerical solution of the dynamic stability problem for structural forms made of reinforced ribbed composite materials. This is a complex problem, but currently, there are not many published research results to determine the critical force, the stability domain of the structure and the influence of composite tendons on the stability of the structure.

This paper shows the results of using the finite element method and the stability standard of the periodic coefficient linear differential equation system to solve the dynamic stability problem of thin plates made of composite materials. Reinforcing ribs are subjected to cyclic loads acting in the plate plane.

2. GOVERNING EQUATIONS

Consider a rectangular laminated composite plate with reinforcing ribs that run parallel to the plate's edges. Each layer of the plate and the ribs is made of the same material and is arranged in a way that makes the average face of the plate symmetrical. The material of each layer is a homogeneous composite, including the base material and the fiber reinforcement. The problem model is shown in Fig. 1.

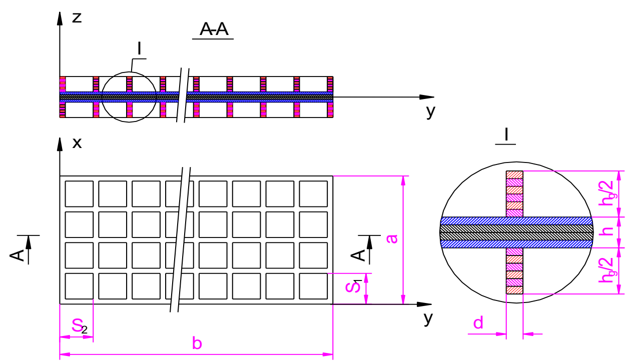

Fig. 1. The model of reinforced composite plate

The plate subjected to bending due to time-varying loads in the mean plane is described by the finite element method by a system of equations as follows [14,15]

$$[M_u]\{\ddot{q}\} + ([K_u] + [K_G(t)])\{q_u\} = 0, \tag{1}$$

where $\{q_u\} = \{w_1\varphi_{x1}\varphi_{y1} \quad \ldots \quad w_n\varphi_{xn}\varphi_{yn}\}$ is the bending displacement vector of the nodes, n is the total number of nodes, $[M_u]$ is the mass matrix, $[K_u]$ is the bending stiffness matrix, $[K_g]$ is the geometric stiffness matrix which changes with time t.

To set up the geometric stiffness matrix in the formula (1), consider plate oscillation subjected to harmonic load T acting in the plate plane as follows

$$[M_f]\{\ddot{q}_f\} + [K_f]\{q_f\} = \{F(t)\}, \tag{2}$$

where $\{q_f\} = \{u_1v_1 \quad \ldots \quad u_nv_n\}$ is the node displacement vector in the plane, $[K_f]$, $[M_f]$ are the stiffness matrix and the mass matrix of the plate in the planar problem, $\{F(t)\}$ is the load vector. The cyclic load vector $\{F(t)\}$ is represented as

$$\{F(t)\} = \{F_0\} + \sum_{k=1}^{N}\{F_k\}\cos kpt, \tag{3}$$

where $p = \dfrac{2\pi}{T}$ is the fundamental frequency. Then the stable forced oscillation has the following form: $\{q_f(t)\} = \{a_0\} + \sum\limits_{k=1}^{N}\{a_k\}\cos p_k t$. The stress at the center of each element is calculated through the node displacement vector

$$\{\sigma\}^e = \{\sigma_x\sigma_y\tau_{xy}\}^e = [D_f]^e[B_f]^e\{q_f\}^e = [D_f]^e[B_f]^e\left(\{a_0\}^e + \sum_{k=1}^{N}\{a_k\}^e\cos p_k t\right). \tag{4}$$

From the stress components in formula (4), the geometric stiffness matrix of the plate has the form

$$[K_G(t)] = [K_{G0}] + \sum_{k=1}^{N}[K_{Gk}]\cos p_k t. \tag{5}$$

The global matrix of the composite plate $[K_u]$, $[K_g]$, $[K_f]$, $[M_u]$, $[K_f]$ are determined from the element stiffness matrix of the composite plate [15]

$$[K_u] = \sum[K_{ue}],\ [M_u] = \sum[M_{ue}],\ [K_f] = \sum[K_{fe}],\ [M_f] = \sum[M_{fe}],\ [K_G] = \sum[K_{Ge}]. \tag{6}$$

2.1. Composite plate element

- Determining $[K_{ue}]$

Considering the rectangular element of the composite plate subjected to bending, at each node there are 3 degrees of freedom (Fig. 2(a)). In this paper, the Kirchhoff plate theory is used to describe the displacement field of the structure.

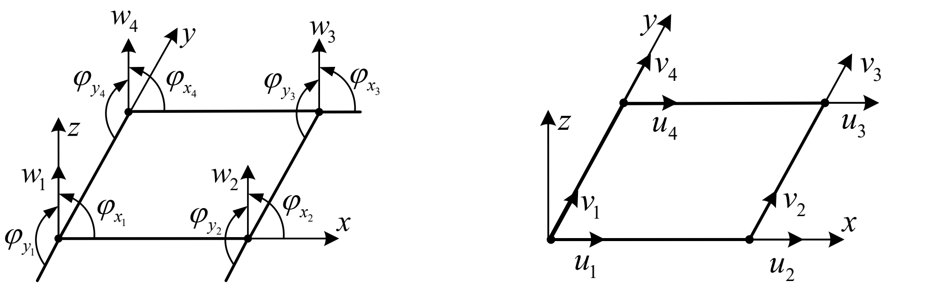

(a) Bending plate (b) Compression plate in the mean plane

Fig. 2. Composite plate element

The node displacement vector and the node load vector of the element are defined as

$$\{q_u\}_e = \left\{ \begin{array}{ccccccc} w_1 & \phi_{x1} & \phi_{y1} & \ldots & w_4 & \phi_{x4} & \phi_{y4} \end{array} \right\}^T. \tag{7}$$

The deflection at a point within the element is determined through the element's node displacements as follows

$$w_0 = [L_w] \{q_u\}_e^T, \tag{8}$$

where $[L_w]$ is the shape function matrix in bending.

$$[L_w] = \left[\begin{array}{ccccccc} N_{u1} & N_{u2} & N_{u3} & \ldots & N_{u10} & N_{u11} & N_{u12} \end{array} \right], \tag{9}$$

where N_{u1} $(i = 1, \ldots, 12)$ is the shape functions in bending [3].

The element's stiffness matrix is determined by the formula [14,15]

$$[K_{ue}] = \int_S [B_u]^T [D_u] [B_u] \, \mathrm{d}S, \tag{10}$$

with $[B_u]$ is the matrix obtained from the differential of shape functions for the bending problem. $[D_u]$ is the matrix of bending stiffness constants of the composite plate, which is determined as follows [16]

$$[D_u] = \left[\begin{array}{ccc} D_{11} & D_{12} & D_{16} \\ D_{12} & D_{22} & D_{26} \\ D_{16} & D_{26} & D_{66} \end{array} \right], \; D_{ij} = \frac{1}{3} \sum_{k=1}^{n} Q_{ij} \left(z_{k+1}^3 - z_k^3 \right), \; (i,\, j = 1, 2, 6). \tag{11}$$

- Determining $\left[K_{ge}^0 \right]$

The components of the matrix $[K_{Ge}]$ are determined as follows [15]

$$\left(K_{ij}\right)_G^e = \int_S \left[N_{0x} \frac{\partial [L_w]}{\partial x} \frac{\partial [L_w]^T}{\partial x} + N_{0y} \frac{\partial [L_w]}{\partial y} \frac{\partial [L_w]^T}{\partial y} + 2N_{0xy} \frac{\partial [L_w]}{\partial x} \frac{\partial [L_w]^T}{\partial y} \right] \mathrm{d}S, \tag{12}$$

where N_{0x}, N_{0y}, N_{0xy} are the internal membrane force components that result when solving the planar problem (2).

- Determining $\left[K_{fe}\right]$

Node displacement vector

$$\left\{q_f\right\}_e = \left\{\begin{array}{cccccccc} u_1 & v_1 & u_2 & v_2 & u_3 & v_3 & u_4 & v_4 \end{array}\right\}^T. \tag{13}$$

The stiffness matrix of the composite film element is determined by the formula

$$\left[K_f\right]_e = \int\limits_s \left[B_f\right]^T \left[D_f\right] \left[B_f\right] \mathrm{d}S, \tag{14}$$

with $\left[B_f\right]$ is the matrix obtained from the differential of shape functions for the bearing plate problem in the mean plane. $\left[D_f\right]$ is the matrix of membrane stiffness constants of the composite plate, which is determined as follows [4]

$$\left[D_f\right] = \left[\begin{array}{ccc} A_{11} & A_{12} & A_{16} \\ A_{12} & A_{22} & A_{26} \\ A_{16} & A_{26} & A_{66} \end{array}\right], \; A_{ij} = \sum_{k=1}^{n} Q_{ij}\left(z_{k+1} - z_k\right), \; (i, j = 1, 2, 6). \tag{15}$$

- Determining $[M_{ue}]$

$$[M_{ue}] = \int\limits_S \left\{J_0 \left[L_w\right]^T \left[L_w\right]\right\} \mathrm{d}S, \tag{16}$$

where

$$J_0 = \sum_{k=1}^{n} \rho_k \left(z_{k+1} - z_k\right), \tag{17}$$

with ρ_k is the density of the k^{th} composite layer material.

2.2. Stiffener composite element

For bending and torsion, stiffeners are modeled as composite beam elements, as shown in Fig. 3(a).

The nodal element displacement vector is defined as

$$\left\{q_{gue}\right\} = \left\{\begin{array}{cccccc} w_1 & \theta_{x_1} & \theta_{y_1} & w_2 & \theta_{x_2} & \theta_{y_2} \end{array}\right\}^T. \tag{18}$$

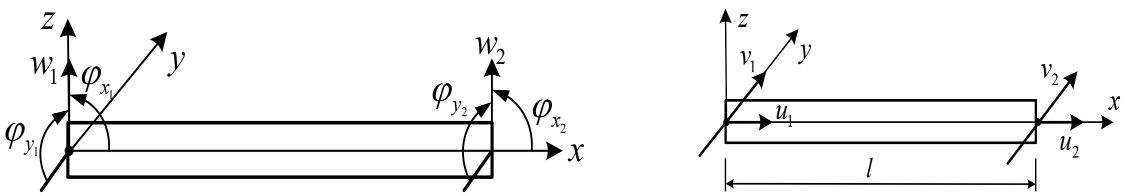

(a) Bending and torsion beam (b) compression beam

Fig. 3. Composite beam element

Stiffness and mass matrix of the bending composite beam element

$$[K_{gue}] = \begin{bmatrix} \dfrac{12E_uJ_y}{\ell^3} & 0 & -\dfrac{6E_uJ_y}{\ell^2} & -\dfrac{12E_uJ_y}{\ell^3} & 0 & -\dfrac{6E_uJ_y}{\ell^2} \\ 0 & \dfrac{G_xJ_x}{\ell} & 0 & 0 & -\dfrac{G_xJ_x}{\ell} & 0 \\ -\dfrac{6E_uJ_y}{\ell^2} & 0 & \dfrac{4E_uJ_y}{\ell} & \dfrac{6E_uJ_y}{\ell^2} & 0 & \dfrac{2E_uJ_y}{\ell} \\ -\dfrac{12E_uJ_y}{\ell^3} & 0 & \dfrac{6E_uJ_y}{\ell^2} & \dfrac{12E_uJ_y}{\ell^3} & 0 & \dfrac{6E_uJ_y}{\ell^2} \\ 0 & -\dfrac{G_xJ_x}{\ell} & 0 & 0 & \dfrac{G_xJ_x}{\ell} & 0 \\ -\dfrac{6E_uJ_y}{\ell^2} & 0 & \dfrac{2E_uJ_y}{\ell} & \dfrac{6E_uJ_y}{\ell^2} & 0 & \dfrac{4E_uJ_y}{\ell} \end{bmatrix}, \tag{19a}$$

$$[M_{gue}] = \begin{bmatrix} \dfrac{13\rho_tF\ell}{35} & 0 & \dfrac{11\rho_tF\ell^2}{210} & \dfrac{9\rho_tF\ell}{70} & 0 & -\dfrac{13\rho_tF\ell^2}{420} \\ 0 & \dfrac{\rho_t\ell J_x}{3} & 0 & 0 & \dfrac{\rho_t\ell J_x}{6} & 0 \\ \dfrac{11\rho_tF\ell^2}{210} & 0 & \dfrac{\rho_tF\ell^3}{105} & -\dfrac{13\rho_tF\ell^2}{420} & 0 & -\dfrac{\rho_tF\ell^3}{140} \\ \dfrac{9\rho_tF\ell}{70} & 0 & \dfrac{13\rho_tF\ell^2}{420} & \dfrac{13\rho_tF\ell}{35} & 0 & -\dfrac{11\rho_tF\ell^2}{210} \\ 0 & \dfrac{\rho_tF\ell J_x}{6F} & 0 & 0 & \dfrac{\rho_tF\ell J_x}{3F} & 0 \\ -\dfrac{13\rho_tF\ell^2}{420} & 0 & -\dfrac{\rho_tF\ell^3}{140} & -\dfrac{11\rho_tF\ell^2}{210} & 0 & \dfrac{\rho_tF\ell^3}{105} \end{bmatrix}. \tag{19b}$$

For compression and bending, stiffeners are modeled as composite bar elements as shown in Fig. 3(b). The node element displacement vector

$$\{q_{gne}\} = \{\, u_1 \quad v_1 \quad u_2 \quad v_2 \,\}^T. \tag{20}$$

Stiffness and mass matrix of the compression composite bar element [3]

$$\left[K_{gne}\right]=\begin{bmatrix}\dfrac{E_mF}{\ell} & 0 & -\dfrac{E_mF}{\ell} & 0\\ 0 & \dfrac{12E_uJ}{\ell^3} & 0 & -\dfrac{12E_uJ}{\ell^3}\\ -\dfrac{E_mF}{\ell} & 0 & \dfrac{E_mF}{\ell} & 0\\ 0 & -\dfrac{12E_uJ}{\ell^3} & 0 & \dfrac{12E_uJ}{\ell^3}\end{bmatrix},\tag{21}$$

$$\left[M_{gne}\right]=\begin{bmatrix}\dfrac{\rho_tF\ell}{3} & 0 & \dfrac{\rho_tF\ell}{6} & 0\\ 0 & \dfrac{13\rho_tF\ell}{35} & 0 & \dfrac{9\rho_tF\ell}{70}\\ \dfrac{\rho_tF\ell}{6} & 0 & \dfrac{\rho_tF\ell}{3} & 0\\ 0 & \dfrac{9\rho_tF\ell}{70} & 0 & \dfrac{13\rho_tF\ell}{35}\end{bmatrix}.$$

According to [16]

$$\begin{aligned}
&E_m=\frac{1}{\Delta_1}\left(A_{22}A_{66}-A_{66}^2\right);\ \Delta_1=A_{11}A_{12}A_{66}+2A_{12}A_{16}A_{26}-A_{11}A_{26}^2-A_{22}A_{16}^2-A_{66}A_{12}^2,\\
&E_u=\frac{12}{h_t^3D_{11}^{\Sigma}},\ D_{11}^*=\frac{1}{\Delta_2}\left(D_{22}D_{66}-D_{26}^2\right),\ G_x=\frac{1}{\beta_th_tb_t^2D_{66}^*},\\
&\Delta_2=D_{11}D_{12}D_{16}+2D_{12}D_{16}D_{26}-D_{11}D_{26}^2-D_{22}D_{16}^2-D_{66}D_{12}^2,\\
&D_{66}^*=\frac{1}{\Delta_3}\left(D_{11}D_{22}-D_{12}^2\right),\Delta_3=D_{11}D_{22}D_{66}+2D_{12}D_{16}D_{26}-D_{11}D_{26}^2-D_{22}D_{16}^2-D_{66}D_{12}^2.
\end{aligned}\tag{22}$$

with b_t, h_t, F, ρ_t are cross-sectional dimensions of the beam, the mass density of the composite material. β_t coefficient depends on the size of the cross-section. J_x and J_y are the moments of inertia of the cross-section with respect to the x-axis, y-axis, respectively; and l is the length of the element.

Using the mode analysis method [14,15]. Then, the solution of equation (1) is found by linear transformation in the form: $\{q_u\}=[V]\{q\}$. $[V]$ is the matrix containing the m first free vibration mode shapes of the bending plate, which are determined from the unrestrained free vibration equation

$$[M]\{\ddot{q}\}+([K]+[G(t)])\{q\}=0,\tag{23}$$

$$[M]=[V]^T[M_u][V],\quad [K]=[V]^T[K_u][V],\quad [G(t)]=[V]^T[K_G(t)][V].\tag{24}$$

When $[V]$ the matrix is normalized to the mass, then $[M]=[E];[K]=[\Omega]$.

The problem is brought back to consider the stability of the solution of the system of m equations for generalized coordinates $\{q\}$

$$\{\ddot{q}\} + ([\Omega] + [G(t)])\{q\} = 0. \tag{25}$$

The resistance matrix is diagonalized as: $[C_u] = \alpha [K_u] + \beta [M_u]$.

Eq. (25) becomes

$$\{\ddot{q}\} + (\alpha [\Omega] + \beta [E])\{\dot{q}\} + ([\Omega] + [G(t)])\{q\} = 0. \tag{26}$$

Thus, the stability study of system (1) is reduced to the reduced system (26). Call the state vector of equation (26)

$$\{x(t)\} = \left\{ \begin{array}{cccccc} q_1(t) & \ldots & q_m(t) & \dot{q}_1(t) & \ldots & \dot{q}_m(t) \end{array} \right\}^T. \tag{27}$$

The equation of state for a time-varying linear system (27) has the form

$$\{\dot{x}(t)\} = [A(t)]\{x(t)\}, \quad \{x_0\} = \{x(0)\}, \tag{28}$$

where is a square matrix of order $2m$. In the particular case under consideration, matrix $[A]$ dependent on time t has the form:

$$[A(t)] = \left[\begin{array}{cc} [0] & [E] \\ -([\Omega] + [G(t)]) & -(\alpha [\Omega] + \beta [E]) \end{array} \right]. \tag{29}$$

3. STABILITY CRITERIA

The general solution of system (28) has the form $\{x(t)\} = [\Phi(t,0)]\{x_0\}$, where $[\Phi(t,0)]$ is called the basic matrix of the system (28). The j^{th} column of this matrix is the j^{th} eigenvalue of the system (28), denoted $\{x(t)\}^{(j)}$, with the initial condition $\{x_0\}^{(j)} = \{x(0)\}^{(j)}$. The stability condition of the system (28) with $[A(t)]$ a periodic matrix T depends on the eigenvalues of the matrix $[\Phi(T,0)]$, the solutions of the equation

$$\det([\Phi(T,0) - \mu [E]]) = 0. \tag{30}$$

Called μ_k is eigenvalues of $[\Phi(T,0)]$, in general they are complex numbers. The stability criteria is stated as follows [17]: *The system is asymptotically stable if every eigenvalue has a modulus of less than 1. If every eigenvalue has a modulus of no more than 1, there is an eigenvalue with a modulus equal to 1.1, the system is marginally stable. Conversely, even a single value μ_k with a modulus greater than 1 makes the system unstable.*

4. NUMERICAL RESULTS

Consider a rectangular composite plate of size $B \times L$ ($B = 100$ cm, $L = 200$ cm), thickness $h = 0.5$ cm, clamped at $y = 0$. The longitudinal and transverse stiffeners are arranged with the distance between the stiffener: $e_x = 20$ cm, $e_y = 40$ cm, the cross-sectional dimension of the stiffener is $b_g \times h_g = 2.0$ cm $\times$ 0.5 cm. The plate is meshed into 30 rectangular elements by 42 nodes, the stiffeners are meshed into 71 elements, the plate is subjected to concentrated forces $P = P_0 \cos \theta t$ as shown in Fig. 4.

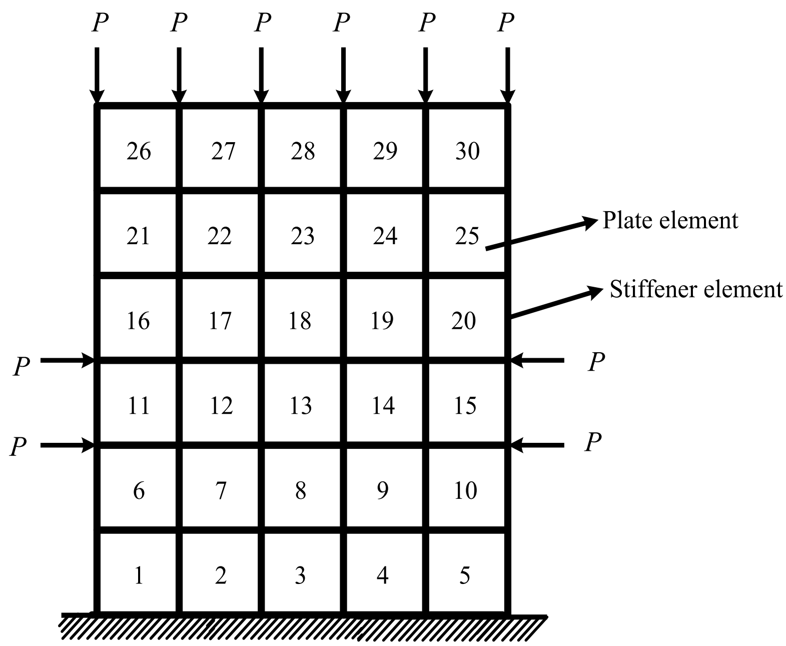

Fig. 4. Mesh diagram of stiffened plate

Composite material parameters for calculation are given in Table 1.

Table 1. Composite material parameters

No	E_c (N/cm^2)	E_n (N/cm^2)	ρ_c (kg/cm^3)	ρ_n (kg/cm^3)	Core coefficient	Core angle (degree)	Layer thickness h_k (cm)
1	39×10^6	7×10^6	0.00263	0.0027	0.4	0	0.1
2	13×10^6	7×10^6	0.00280	0.0027	0.4	60	0.1
3	7.4×10^6	7×10^6	0.00295	0.0027	0.4	90	0.1
4	13×10^6	7×10^6	0.00280	0.0027	0.4	60	0.1
5	39×10^6	7×10^6	0.00263	0.0027	0.4	0	0.1

4.1. Influence of the ply angle

With frequency $\theta = 20\ \dfrac{\text{rad}}{\text{s}}$, P_0 = 4000 N, the results with different values of the core angle of the composite layers are given in Table 2.

Table 2. Influence of the ply angle

Ply angle (degree)	Result
0	Stability
15	Unstabiliy
30	Unstabiliy
45	Unstabiliy
60	Unstabiliy
75	Unstabiliy
90	Stability

The stability of the plate increases when the ply angle is 0 degree and 90 degrees.

4.2. Influence of the ratio of plate thickness and stiffener thickness (h_g/h)

With frequency $\theta = 20\ \dfrac{\text{rad}}{\text{s}}$, P_0 = 4000 N, the stability of the plate with different values ratio of plate thickness and stiffener thickness shown in Table 3.

Table 3. Influence of the ratio of plate thickness and stiffener thickness

h_g/h	Result
0.5	Unstabiliy
0.6	Unstabiliy
0.7	Unstabiliy
0.8	Unstabiliy
0.9	Stability
1.0	Stability
1.2	Stability

The stability of the plate increases as the ratio of plate thickness and stiffener thickness increases (the thickness of the stiffener increases).

4.3. Influence of load amplitude

With frequency $\theta = 20\ \dfrac{\text{rad}}{\text{s}}$, the results with different values of load amplitude as shown in Table 4.

Table 4. Influence of load amplitude

P_0 (N)	Result
4000	Stability
4500	Stability
5000	Stability
5500	Stability
6000	Stability
6500	Stability
7000	Stability
7190	Unstabiliy

When increasing the load amplitude leads to the possibility of dynamic instability of the plate, in the case under consideration, with the load amplitude $P_0 \geq 7190$ N, the plate becomes unstable.

4.4. Influence of load frequency

The influence of the load frequency on the stability of the plate, solve some problems with different load frequencies, with P_0 = 4000 N. The results are shown in Table 5.

Table 5. Influence of load frequency

Load frequency θ (rad/s)	Result
1	Unstability
5	Unstability
10	Stability
20	Stability
30	Stability
40	Stability
50	Stability

With the specific data of the problem, it can be see that with a small load frequency, the plate becomes unstable. Specifically, with Ω = 1 rad/s and Ω = 5 rad/s, the plate will be unstable.

4.5. Determine the buckling domain of the plate with load amplitude and stiffener thickness

Building a stable region of the plate with two variable parameters: Load amplitude P_0 varies from 10 N to 10000 N and stiffener thickness varies from 0 to 1.5 cm. Fig. 5 shows the buckling domain results of the plate. The blue region correspond to the parameters for the plate to be stable, the white region are unstable.

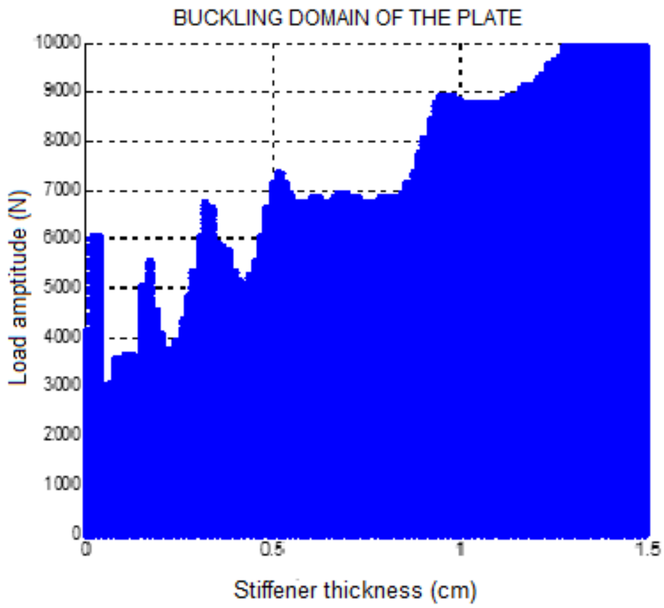

Fig. 5. Buckling domain of the plate

5. CONCLUSIONS

The main results presented in this paper are as follows: Equation for parametric vibration of reinforced stiffener composite plate with geometric stiffness matrix as periodic matrix, using linear transformation by tool shapes. The unimpeded eigenvalues are converted to a system of compact differential equations of periodic coefficients, the basic matrix is established, and the eigenvalue criteria are used to evaluate the dynamic buckling of the reinforced composite plate.

Specific case survey for a rectangular composite plate with reinforced stiffener, clamped on an edge subjected to harmonic loads in the plane of the plate. The numerical results have illustrated the capabilities of the algorithm and the program, and at the same time evaluated the effect of changing the parameters of the reinforcement angle of the layer, the thickness of the stiffener, the load amplitude to the stability of the plate. Through calculations, a buckling domain of the plate has been recognized when changing the load amplitude and stiffener thickness.

DECLARATION OF COMPETING INTEREST

The authors declare that they have no known competing financial interests or personal relationships that could have appeared to influence the work reported in this paper.

FUNDING

This research received no specific grant from any funding agency in the public, commercial, or not-for-profit sectors.

REFERENCES

[1] V. V. Bolotin. *The dynamic stability of elastic systems*. Holden-Day, San Francisco, (1964).

[2] A. H. Sofiyev. The buckling of laminated cylindrical thin shells under torsion varying as a linear function of time. *Turkish Journal of Engineering and Environmental Sciences*, **27**, (4), (2003), pp. 237–245.

[3] J. M. Hutt and A. E. Salam. Dynamic stability of plates by finite elements. *Journal of the Engineering Mechanics Division*, **97**, (1971), pp. 879–899. https://doi.org/10.1061/jmcea3.0001424.

[4] J. Aboudi, G. Cederbaum, and I. Elishakoff. Dynamic stability analysis of viscoelastic plates by Lyapunov exponents. *Journal of Sound and Vibration*, **139**, (1990), pp. 459–467. https://doi.org/10.1016/0022-460x(90)90676-q.

[5] R. Srinivasan and P. Chellapandi. Dynamic stability of rectangular laminated composite plates. *Computers & Structures*, **24**, (1986), pp. 233–238. https://doi.org/10.1016/0045-7949(86)90282-8.

[6] G. Cederbaum. Dynamic instability of shear-deformable laminated plates. *AIAA Journal*, **29**, (1991), pp. 2000–2005. https://doi.org/10.2514/3.10830.

[7] C. Lien-Wen and Y. Jenq-Yiing. Dynamic stability of laminated composite plates by the finite element method. *Computers & Structures*, **36**, (1990), pp. 845–851. https://doi.org/10.1016/0045-7949(90)90155-u.

[8] S. Wang and D. J. Dawe. Dynamic instability of composite laminated rectangular plates and prismatic plate structures. *Computer Methods in Applied Mechanics and Engineering*, **191**, (2002), pp. 1791–1826. https://doi.org/10.1016/s0045-7825(01)00354-1.

[9] J. E. Grady, C. C. Chamis, and R. A. Aiello. Dynamic delamination buckling in composite laminates under impact loading: computational simulation. In *Composite Materials, Fatigue and Fracture, 2nd Symposium*, (1989), pp. 137–149.

[10] R. Sahoo and B. N. Singh. Assessment of dynamic instability of laminated composite-sandwich plates. *Aerospace Science and Technology*, **81**, (2018), pp. 41–52. https://doi.org/10.1016/j.ast.2018.07.041.

[11] P. Dey and M. K. Singha. Dynamic stability analysis of composite skew plates subjected to periodic in-plane load. *Thin-Walled Structures*, **44**, (2006), pp. 937–942. https://doi.org/10.1016/j.tws.2006.08.023.

[12] J. Moorthy, J. N. Reddy, and R. H. Plaut. Parametric instability of laminated composite plates with transverse shear deformation. *International Journal of Solids and Structures*, **26**, (7), (1990), pp. 801–811. https://doi.org/10.1016/0020-7683(90)90008-j.

[13] A. Chakrabarti and A. H. Sheikh. Dynamic instability of imperfect laminated sandwich plates with in-plane partial edge load. *Latin American Journal of Solids and Structures*, **7**, (4), (2010), pp. 457–474. https://doi.org/10.1590/s1679-78252010000400006.

[14] K. J. Bathe and E. L. Wilson. *Numerical methods in finite element analysis*. Prentice - Hall, Inc, (1976).

[15] R. H. Galager. *Finite element analysis*. Prentice - Hall, Inc., Englewood Cliffs, New Jersey, (1975).

[16] T. I. Thinh. *Composite material: Mechanical and structural analysis*. Vietnam Education Publishing House, (1994). (in Vietnamese).

[17] P. C. Müller and W. Schiehlen. *Linear vibrations*. Anh, N. D. (Translator), Construction Publishing House, Hanoi, (1997). (in Vietnamese).